

# NANOINDENTATION MEASUREMENTS OF AUSTENO-FERRITIC STAINLESS STEEL SUBMITTED TO HYDROGEN CHARGING

A. Glowacka, M.J. Wozniak and W.A. Swiatnicki

Warsaw University of Technology, Department of Materials Science & Engineering, Woloska 141, 02-507 Warsaw, Poland

Received: November 9, 2004

**Abstract.** The changes of nanohardness as a result of cathodic hydrogen charging of austeno-ferritic stainless steel was investigated. As the hydrogen behaves differently in the ferrite ( $\alpha$ ) and austenite ( $\gamma$ ) phases, the hardness variation of both  $\alpha$  and  $\gamma$  grains before and after hydrogen charging were measured. The nanoindentation measurements using the Atomic Force Microscope were performed. Three various states of samples were examined: initial state, just after hydrogen absorption and after hydrogen desorption. It was shown that there are distinct changes of nanohardness between every state and each phase. Generally, the nanohardness of the  $\gamma$  phase is higher than in case of the  $\alpha$  phase. The increase of nanohardness of both phases after hydrogen absorption and its decrease after hydrogen desorption was observed and interpreted in terms of microstructural changes.

## 1. INTRODUCTION

It is well known that the most distinct changes of the material microstructure bring about by hydrogen occur mostly in thin superficial layer. The microhardness measurements performed by Lublinska [1] revealed no difference before and after hydrogenation process. However, it does not mean that there are no microstructural changes introduced by hydrogen. Our earlier studies using transmission electron microscope (TEM) [2,3] revealed great microstructure changes (i.e. an increase of dislocation and stacking faults density) in thin foils affected by hydrogen. It seemed that a layer which is influenced by hydrogen is so thin, that it is difficult to find an appropriate technique sensible enough to characterise her properties. In order to do this we took advantage of atomic force microscope (AFM) nanoindentation module.

## 2. EXPERIMENTAL

The material used in this study was Cr23-Ni5-Mo3 austeno-ferritic duplex stainless steel (chemical composition in wt.%: 0.026C, 0.35Si, 1.57Mn, 5.43Ni, 22.94Cr, 2.75Mo, 0.164N, 0.001S, 0.021P, 0.012Al).

The material was subjected to a thermo-mechanical treatment in order to produce the same volume fraction of austenite and ferrite, and special orientation relationships (ORs) between the  $\alpha$  and  $\gamma$  phases [4].

Then, the samples were machined to reduce their diameter to 3 mm and next sliced to 0.2 mm thick discs using a wire saw. Finally, they were polished by two-sided electrolytic thinning.

Hydrogen charging of the specimens were carried out electrolytically at room temperature in a 0,1M  $H_2SO_4$  aqueous solution with an addition of 10mg/l

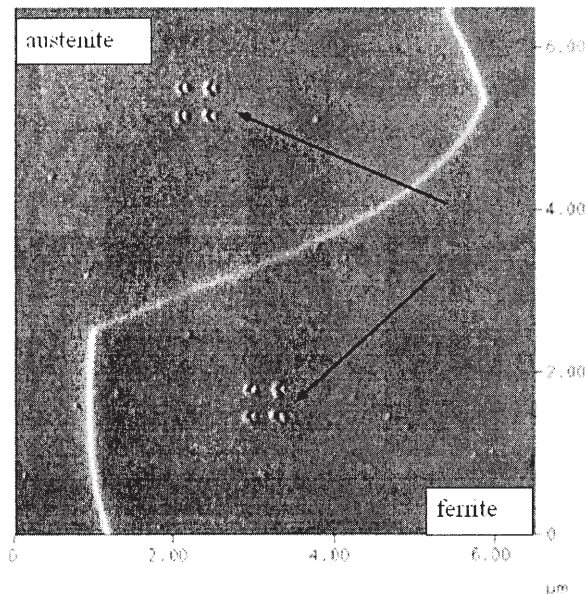


Fig. 1. Nanoindentations performed in both phases.

of a hydrogen entry promoter ( $\text{As}_2\text{O}_3$ ). A current density of  $20 \text{ mA/cm}^2$  was applied between the specimen and a platinum anode.

The nanoindentation measurements of the steel samples were examined with a Multi Mode AFM NanoScope IIIa Digital Instruments. There were tested three various states of samples: 1) at the initial state, before hydrogen charging; 2) just after hydrogen charging; 3) after hydrogen desorption.

The AFM was operated in the nanoindentation mode. Before indentation, the topographic image (in Tapping Mode) was collected. This image of sample surface was performed in order to locate the desired area for the indentation. After selection of desired area, the indentation was executed. During indentation a kind of force-displacement curve was recorded. For better statistics few indentations were performed simultaneously. After indentation the topographic image was collected one more time in order to measure indentation holes. From the size of the indentation holes and force-displacement curve the hardness data could be extracted. The important factor was that the indentation and image collection were performed using only one tip probe.

Indentation probe consisted of a diamond tip, mounted on a metal foil cantilever. The diamond tip was sharp enough to provide good image resolution (radius of the curvature  $25 \text{ nm}$ ). The tip of the probe used during the experiment was the Berkovich diamond triangular pyramid (pyramid formed by  $\{111\}$  surface of the diamond single crystal). The param-

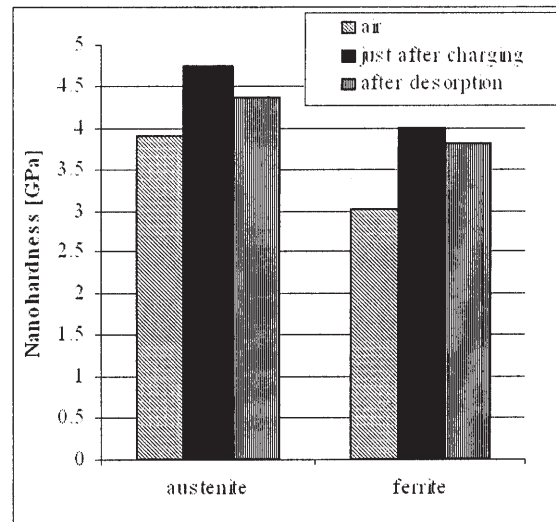


Fig. 2. Nanoindentation hardness variations in ferrite and austenite.

eters of the probe were: cantilever length  $356 \text{ mm}$ , spring constant  $272.4 \text{ N/m}$ , resonant frequency  $68 \text{ kHz}$ . The microscope was calibrated on sapphire sample before the set of experiments. In each experiment four indentations were performed at once (see Fig. 1).

### 3. RESULTS AND DISCUSSION

Nanoindentation measurements allowed us to investigate the nanoindentation hardness of austenitic-ferritic steel before and after cathodic hydrogen charging. At first, we determined the difference between austenite and ferrite phases. It was proved that initially, the  $\gamma$  phase reached  $3.91 \text{ GPa}$ , being 23% harder than  $\alpha$  phase ( $3.01 \text{ GPa}$ , see Fig. 2).

Firstly, it was worth to mention about the extremely high values of obtained nanoindentation hardness. Johansson *et al.* [5] which performed nanoindentation measurements of duplex steel received similar rank of values:  $3.9 \text{ GPa}$  for  $\alpha$  phase, and  $4.2 \text{ GPa}$  for  $\gamma$  phase. The differences in nanoindentation hardness values may result from different chemical composition of the investigated steels.

The influence of hydrogen cathodic charging on the change of steel hardness was well visible (see Fig. 2 and Fig. 3). The nanoindentation hardness of both phases was increased. It seemed interesting that the growth was relatively higher in the case of ferrite. It can be explained by the fact that the hydrogen induced much more severe and homogeneous microstructure changes in the  $\alpha$  phase than in the  $\gamma$  phase. Our earlier observations using TEM [2,3] revealed

huge increase of dislocations density, and strong and uniform ferrite grain refinement. In the  $\gamma$  phase we observed the appearance of stacking faults, but the overall defects density was lower than in the  $\alpha$  phase.

After hydrogen desorption the decrease of nanohardness of both phases was observed. This is caused firstly by material relaxation after hydrogen desorption from the metal atomic network, and secondly by the annihilation of reversible defects generated during hydrogenation process. The drop of ferrite nanohardness was smaller, but it was austenite which was finally much more hard. Despite of hydrogen desorption, the hardness of both phases remained higher than initially. The remaining high nanohardness values was connected with the existence of irreversible microstructure changes provoked by hydrogen.

It was interesting that the nanohardness of  $\gamma$  phase dropped even there was a martensite formation after several hours after hydrogenation process. It showed us that martensitic transformation had small influence on austenite hardness. It is worth to mark out that the nanoindentation in  $\gamma$  phase was performed outside martensitic laths. Moreover, the decrease of hardness was higher in the case of  $\gamma$  phase than the  $\alpha$  phase. This phenomenon could be easily explained knowing the different behaviour of hydrogen in each phase: the diffusivity of hydrogen in the  $\alpha$  and  $\gamma$ -phases, determined for a similar Cr25-Ni5-Mo DSS amount respectively to  $D_\alpha = 1.5 \cdot 10^{-7} \text{ cm}^2/\text{s}$  [6] and  $D_\gamma = 1.2 \cdot 10^{-12} \text{ cm}^2/\text{s}$  [7]. Also well known higher solubility of hydrogen in  $\gamma$  phase ( $C_\alpha = 3.6 \cdot 10^{-4} \text{ mol}/\text{cm}^3$  and  $C_\gamma = 9.4 \cdot 10^{-3} \text{ mol}/\text{cm}^3$  [8]) enabled higher hydrogen absorption and in consequence introduced more stresses into the crystalline network. After hydrogenation process these stresses gradually declined as a result of a slow hydrogen desorption; this process took several hours because of low diffusivity of hydrogen in fcc  $\gamma$  phase). On the other hand very low solubility of hydrogen in  $\alpha$  phase prevented hydrogen absorption, so there were no nanohardness change after hydrogen desorption from the material. It meant also that the microstructural changes in ferrite were more stable.

#### 4. CONCLUSIONS

The use of atomic force microscope nanoindentation module permitted us to reveal the hydrogen induced nanohardness variation which occur mostly in the thin surface layer of the material. It was possible to measure nanohardness changes before and after hydrogen charging. The observed effects may be

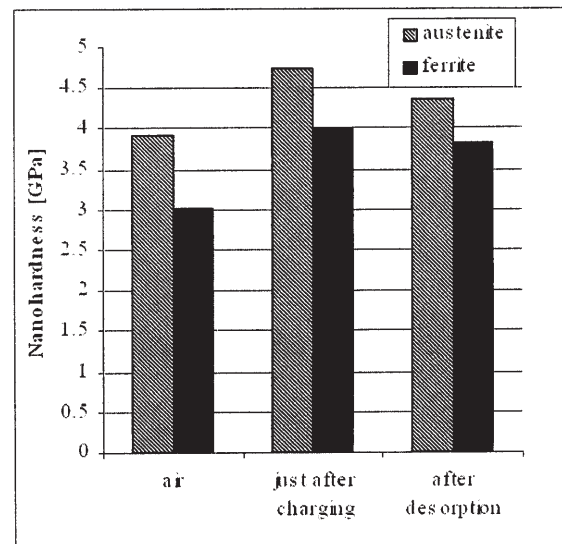


Fig. 3. Nanohardness variations in ferrite and austenite in function of samples state.

explained by the microstructural and phase transformation taking place in the external layer of the austeno-ferritic steel during cathodic hydrogen charging, and after hydrogen desorption from the material.

#### ACKNOWLEDGEMENT

This work was supported by Warsaw University of Technology.

#### REFERENCES

- [1] K. Lublinska, *PhD Thesis* (Warsaw University of Technology, Warsaw 2003).
- [2] A. Glowacka and W.A. Swiatnicki // *J. Alloys and Compounds* **356-357** (2003) 701.
- [3] A. Glowacka and W.A. Swiatnicki // *Mater. Chem. and Phys.* **81** (2003) 496.
- [4] G. Nolze, *Internal report*.
- [5] J. Johansson, M. Oden and X.-H. Zeng // *Acta Mater.* **47** (1999) 2669.
- [6] E. Owczarek and T. Zakroczymski // *Acta Mater.* **48** (2000) 3059.
- [7] T. Zakroczymski and E. Owczarek // *Acta Mater.* **5** (2002) 2701.
- [8] E. Owczarek and T. Zakroczymski // *Ochrona przed Korozją XLII* (1999) 467, in Polish.